SHEAR STRENGTH EVALUATIONS OF REINFORCED CONCRETE BEAMS

N. Hawkins,
Department of Civil Engineering, University of Illinois at Urbana-Champaign,
U.S.A.
S. Kono,
Department of Architecture and Civil Engineering, Toyohashi University of
Technology, Japan

Abstract
Controlled displacement mixed mode loading tests were made on three point
bend specimens with offset notches and exterior steel bars. Variables in the
tests were the concrete strength, the level of prestress in the bars and the area
of the bars. Detailed measurements were made of crack mouth opening and
crack mouth sliding displacements, the progress of the crack with increasing
displacements and the value of the centrally applied load and its displacement.
The findings from that investigation are compared with results from
theoretical and experimental investigations by others into the effects of
restrained shrinkage, and the shear behavior of reinforced concrete beams and
shear friction type specimens. Those comparisons are used to identify some
key factors that must be considered when using fracture mechanics
approaches to predict the shear strength of reinforced concrete beams.
Key words: Mixed mode cracking, shear strength

1 University of Illinois Mixed Mode Fracture Tests

In order to investigate the use of fracture mechanics concepts to predict the shear strength of concrete beams, tests were conducted at the University of Illinois on 43 three point bend (TPB) specimens, 51 x 127 mm in section and centrally loaded on a 508 mm span. Details of a typical test specimen are shown in Fig.1. The beams had 25.4 mm deep and 2.5 mm wide notches sawn into the bottom of the beam and offset 51 or 102 mm from its center. A unique feature of those tests was the use of prestressed steel bars placed either side of the test specimen, positioned 12.7 mm above the bottom of the beam and anchored against steel plates extending across the width of the ends of the beam. The existence of such bars was found essential to proper simulation in the tests of the crack curving behavior observed for flexure-shear cracking of reinforced or prestressed concrete beams. Without such bars the crack propagated through the depth of the beam at a constant angle to the notch and did not exhibit curving behavior.

In addition to the offset of the notch, the effect of three other variables were examined in the tests: the compressive strength of the concrete, 15.5 or 58 MPa; the ratio of the cross-sectional area of the external steel bars to the sectional area of the specimens, 0.5 or 2.0%; and the initial prestress force in the bars, 890 or 1780 KN.

Measurements were made of the load line displacement, (LLD), the crack mouth opening displacement, (CMOD), the crack mouth sliding displacement, (CMSD), the applied central load, the forces in the external bars, the location of the crack front on the surface of the beam with increasing load, and the profile of the crack through the transverse width of the beam with increasing load. To determine the location of the crack front with increasing load, strain
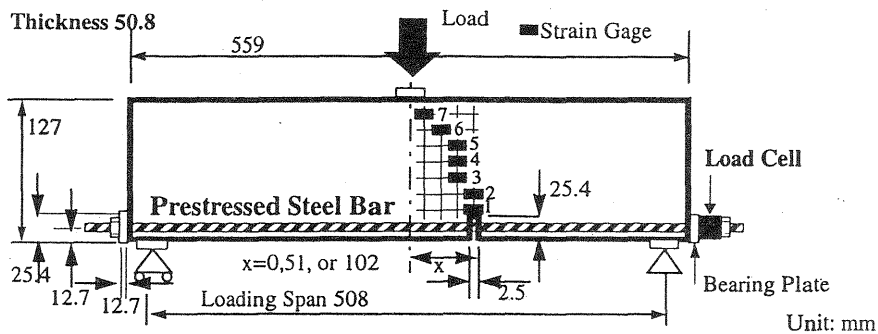

Fig. 1. Geometry and instrumentation for mixed mode fracture tests

gauges were attached to the surface of the beam in accordance with the grid shown in Fig. 1. The profile and progress of the crack through the transverse width of the beam were determined for selected specimens by dye penetration techniques. Specimens were loaded to failure at a fixed rate that was initially 60×10^{-6} mm/sec and increased to 500×10^{-6} mm/sec after the LLD exceeded 0.1 mm. Testing was discontinued when the LLD reached 0.25 mm.

Details of the results for five typical specimens, the results of the dye penetration tests, and the procedures used for numerical simulation of the results have been described in Kono et al. (1995). Comprehensive details of the test specimens, instrumentation, test procedures and numerical simulation investigations of the test results are given in Kono, (1995).

Load-CMOD relationships for five specimens, typical of the test results, are shown in Fig. 2. Letters A and B at the end of the specimen designation indicate duplicate specimens. Specimen 400 had no external constraints. Specimens 412 and 414 had external bars of the same size with the initial prestress force being higher for 414 than 412. For the 414 specimens the height of the crack at a given CMOD is indicated by a solid circle. The thick broken lines labeled 12 and 14 indicate the responses predicted for 412 and 414, respectively, when tied arch action is assumed to govern behavior after inclined cracking.

Measured LLD and CMSD-CMOD relationships for TH414A, typical of the results for all the test specimens, are shown in Fig. 3. CMSD values at a given CMOD were always smaller than CMOD values. Ratios were about
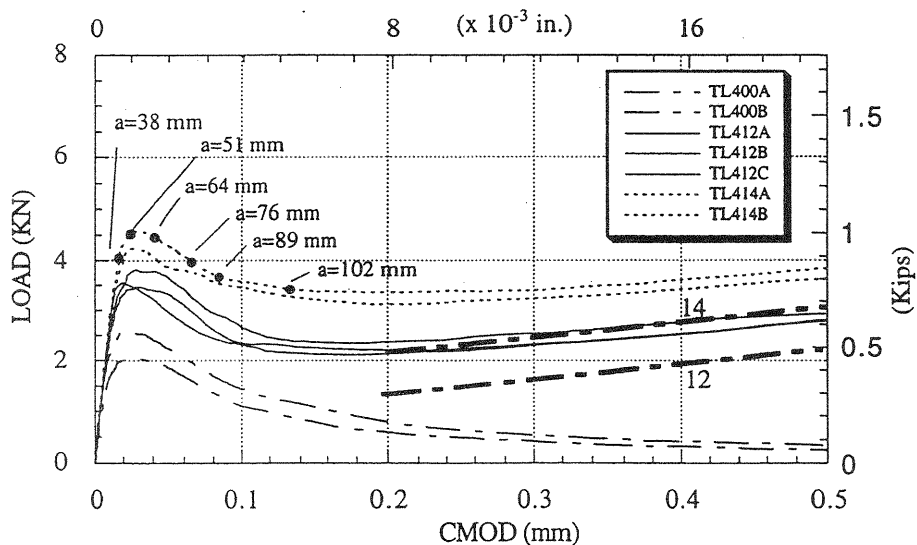

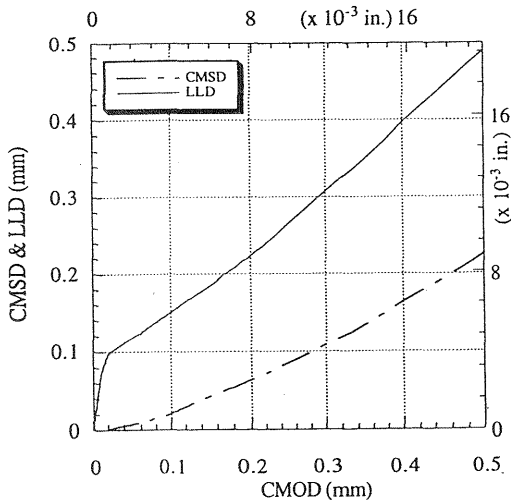Fig. 2. Load-CMOD relationships for typical mixed mode fracture tests

Fig. 3. Typical CMSD and LLD-CMOD relationships

0.2 for CMODs of 0.1 mm and less and increased with the arch action at higher CMODs to a ratio of 0.45 at a CMOD value of 0.5 mm. The slope of the LLD versus CMOD relationship was nearly constant at 45° except prior to the development of the maximum load at about 0.02 mm CMOD.

The numerical simulation approach used to study the test results is shown in Fig. 4. The propagation of a discrete crack, tracing the path of the observed crack and embedded in the two dimensional finite element mesh of Fig. 5, was used to study the effects of optimization of each of the parameters shown in Fig. 4 for the test data from 10 typical specimens. Shown by diagonal crosses in Fig. 2 are the crack height, CMOD and load predicted for the TH414 specimens for the best simulation of crack progress that could be obtained through such finite element modeling and optimization procedures.
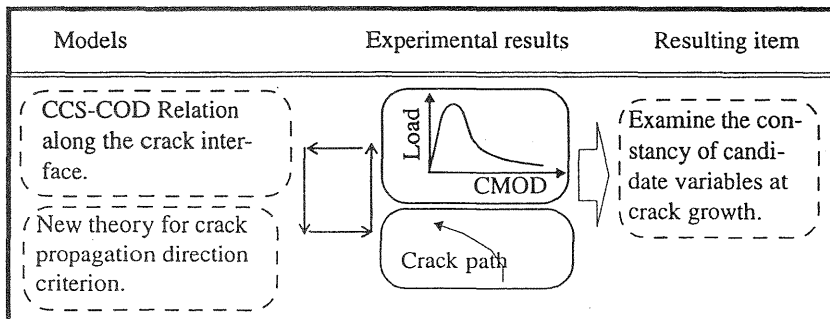

Fig. 4. Modeling concept for numerical simulation studies

1432

2D Modeling

Load line displacement (LLD)

Fine mesh area

Bar force

Bar force
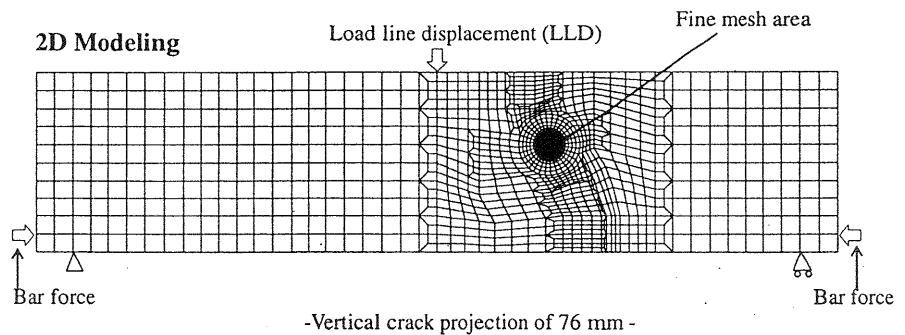
-Vertical crack projection of 76 mm -

Fig. 5. Typical finite element mesh for numerical simulation studies

Principal findings from the physical experiments were:
1. The higher the constraints provided by the external bars and the lower the concrete strength the greater was the initial inclination of the crack with respect to the axis of the notch. Excessive constraints, however, resulted in Mode I crack formation at the center of the beam prior to inclined cracking from the notch.
2. The curvature of the crack reflected the degree of the Mode II component in the mixed mode conditions.
3. Cracks extended at least 13 mm from the notch tip before the peak load was reached and once the crack had penetrated through 80% or more of the beam depth, tied arch behavior dominated the response.

Principal findings from the numerical simulations were:
1. Crack propagation direction is a local parameter useful for determining fracture process zone characteristics such as the crack closing stress, (CCS), versus crack opening displacement, (COD), relationship.
2. There was no need to include a crack sliding stress, (CSS), - COD relationship for the simulated response to match measured local parameters such as CMOD, crack path, etc. Thus, for determination of crack propagation direction there is no need to include the aggregate interlock effects commonly assumed responsible for providing the majority of the shear capacity of a reinforced concrete beam.
3. To predict crack propagation direction the overall stress field in a body of about 15 mm radius, and centered the crack tip, needed to be utilized rather than the stress field centered on the mathematical position of the crack tip.
4. The crack propagation direction was moderately, but not markedly sensitive, to the CCS-COD relationship used in numerical simulations.
5. No unique variable could be found that controlled stable crack growth.

2 Shear Strength Predictions

Many recent studies have shown that the nominal shear stress at failure, for beams with longitudinal tension reinforcement only, varies with the square root of the effective depth of the member as well as with the square root of the concrete compressive strength, Mihashi et al. (1994). The variation with depth for a given test series can be correctly predicted using fracture mechanics concepts. Walraven (1995) has provided an excellent recent summary of knowledge concerning the effects of size on shear strength for beams with longitudinal tension reinforcement only and shown that a reasonable descriptor of that effect is given by S where

$$S = (1 + d/100)^{-\frac{1}{2}} \qquad\qquad (1)$$

d is the effective depth of the member in millimeters and S has a limiting value at d equal to 1500 mm.

However, for beams with web reinforcement, or beams with longitudinal face reinforcement, the dependence of the nominal shear stress at failure on beam depth is considerably smaller than that described by Eq. 1. For example, Walraven's results for deep beams (1995) show that even with minimum amounts of web reinforcement the shear strength increases much more rapidly than predicted by truss analogy concepts. Collins et al. (1996) have shown that for beams with orthogonal longitudinal and web reinforcement the shear strength has little dependence on beam depth and can be closely predicted using compression field theory.

The surface of an inclined crack causing failure in a high strength concrete member is considerably smoother than that of a crack causing failure in a normal strength concrete member. In the former, cracks propagate through the coarse aggregate, rather than around them. Consistent with the concept that aggregate interlock is a major source of shear transfer across inclined cracks, Collins and Kuchma (1998) have shown that for 450 mm deep beams with 0.81% reinforcement, as the concrete strength increases from 37 to 98 MPa, there is a 27 % decrease in the shear strength from 0.16 to 0.117 of the square root of the concrete compressive strength.

Collins and Kuchma also found that when longitudinal face reinforcement is used its effects are significantly greater for high strength than normal strength concrete. For longitudinal face steel equal in amount to 67 % of the main longitudinal steel in a beam with 1.11% reinforcement, the shear strength increased 47 % for a 98 MPa concrete and only 24 % for a 37 MPa concrete, compared to the strengths for beams without face steel.

In American practice, in a beam with shear reinforcement, a portion of the shear is assumed to be provided by the concrete and the remainder by the shear reinforcement. The shear strength provided by the concrete is assumed to be the same for beams with and without shear reinforcement and is taken as the shear causing significant inclined cracking. However, in a beam without shear reinforcement, the shear causing inclined cracking is not necessarily the same as the shear strength for failure . Although most beams without web reinforcement can carry a shear greater than that for inclined cracking, some cannot and fail simultaneously with cracking.

The observations suggest a need to differentiate between conditions at inclined crack initiation and those associated with inclined crack propagation. Inclined cracks typically develop out, or are initiated by flexural cracks. For that action the nature of the effective CCS-COD relationship for the concrete in tension should be important. However, for inclined crack propagation the effect of the reinforcement on equilibrium is likely to be important.

3 Conditions at inclined crack initiation

When an analysis is made of crack development it is customary to ignore any residual stress condition existing in the member. For the simulations of Fig. 2 the best agreement was obtained with a CCS-COD relationship that decreased linearly with increasing COD from 1.4 MPa at crack initiation to zero at a COD of 0.05 mm. However, in the corresponding physical experiments care was taken to keep to a minimum any effects of shrinkage. Therefore there should have been almost no residual stresses due to concrete drying. By contrast, for shear strength tests of concrete beams it is generally assumed that shrinkage and creep do not affect the result and therefore those variables are not controlled.

Clark and Spiers (1978) have reported tests to failure on reinforced concrete beams and obtained detailed data on moment-average strain relationships for the extreme tension and compression fibers, for the tensile reinforcement, and for curvatures in the constant moment region. Seven beams pairs of constant width and variable depth and reinforcement properties were tested. Kaklauskas et al. (1997) derived directly from that data effective tensile stress-strain curves for the concrete. A layered model of the cross section of each beam was used to compute internal forces and then the effective stress-strain curves that gave optimum agreement with the test results. The stress-strain results derived for each load stage in the physical tests were used as input for the analysis of each subsequent load stage. The computed curves are
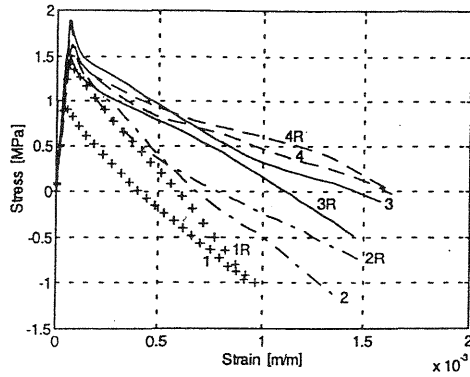
Fig. 6. Tensile stress-strain curve variation with reinforcement ratio

shown in Fig. 6. Beams 1 and 1R, 2 and 2R, 3 and 3R, 4 and 4R contained 1.95%, 1.27%, 0.79% and 0.45 % reinforcement, respectively. It can be seen that the tensile stress for a given post-peak strain increased progressively as the reinforcement ratio decreased. Maximum stresses for beams with large reinforcement ratios were considerably less than the separately measured tensile strength of the concrete. Further, for beams with large reinforcement ratios the effective stress became compressive at large strains. Such results imply that significant tensile stresses are present in the concrete at the start of test due to the reinforcement restraining shrinkage.

Bullington (1991) tested double cantilever beam fracture specimens with and without reinforcing bars crossing a precast starter notch. The geometry of the specimens is shown in Fig.7. Displacement controlled tensile loads
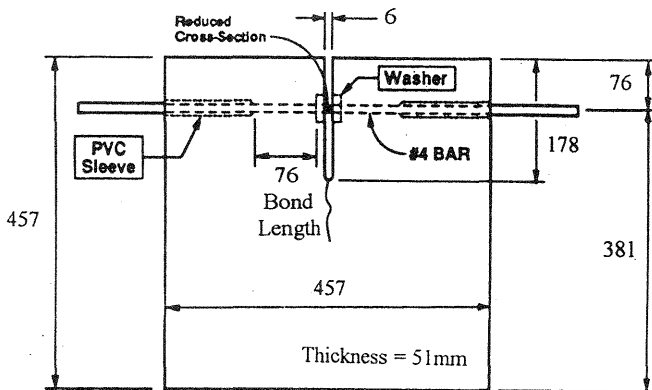

Fig. 7. Bullington's DCB specimens
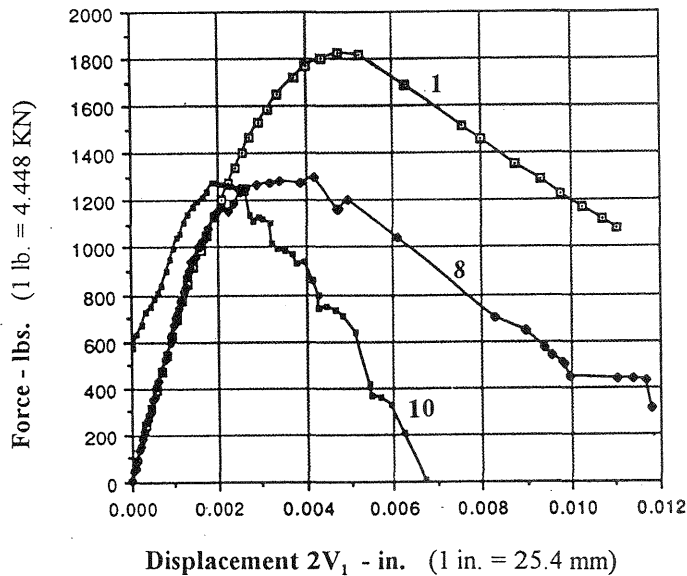
Displacement $2V_1$ - in. (1 in. = 25.4 mm)

Fig. 8. Computed tensile force - $2V_1$ relationships from Bullington's tests

were applied to the protruding ends of the reinforcing bars, crack lengths measured using replica films, and CODs measured at the exterior edge ($2V_1$) and at the initial crack tip. Specimens were moist cured until one day before test. Computed concrete force-$2V_1$ results are shown in Fig.8. Curve 1 is for a specimen where the reinforcing bar never crossed the precast crack and is the result for a plain concrete CLWL-DCB specimen. For curve 8 the bar crossing the notch was cut at the notch immediately prior to testing. There was a decrease in the peak tensile force that could be developed and the slope of the post-peak force-$2V_1$ curve duplicated that for the plain concrete specimen. It was as if specimen 8 had been pretensioned with a force of 534 lbs (2375 KN). That decrease in capacity was due shrinkage of the concrete causing compression in the reinforcement and tension in the concrete. The concrete tension created, in turn, creep strains in the concrete. Cutting the reinforcement released the compression in the bar and the balancing elastic stress in the concrete. However, it could not release the creep strain and that strain gave rise to a pseudo 534 lb force. For test 10 the bar was of the same size as for test 8 but continuous across the notch. The creep locked in a compressive force that did not begin to release until the applied tension exceeded that force. Then once cracking began at the notch tip the residual force between the concrete and steel could not be contained and gradually transferred out of the specimen and into the test frame. That transfer caused a decrease in force with increasing $2V_1$ values greater than for the plain

specimen and the specimen with a cut bar. Clearly CCS values in the FPZ are strain rather than stress dependent and to accurately assess the load for crack initiation account needs to be taken of restrained creep and shrinkage effects.

4 Conditions associated with inclined crack propagation

To examine aggregate interlock effects, Walraven and Reinhardt (1981) made tests on precracked shear-friction specimens. They varied the type of reinforcement crossing the shear plane, using either external bars or 8 mm diameter embedded bars with and without 40 mm long soft sleeves across the shear plane. Typical results are shown in Fig. 9 for specimens with the soft sleeves and the external bars, respectively. Measurements were made of the
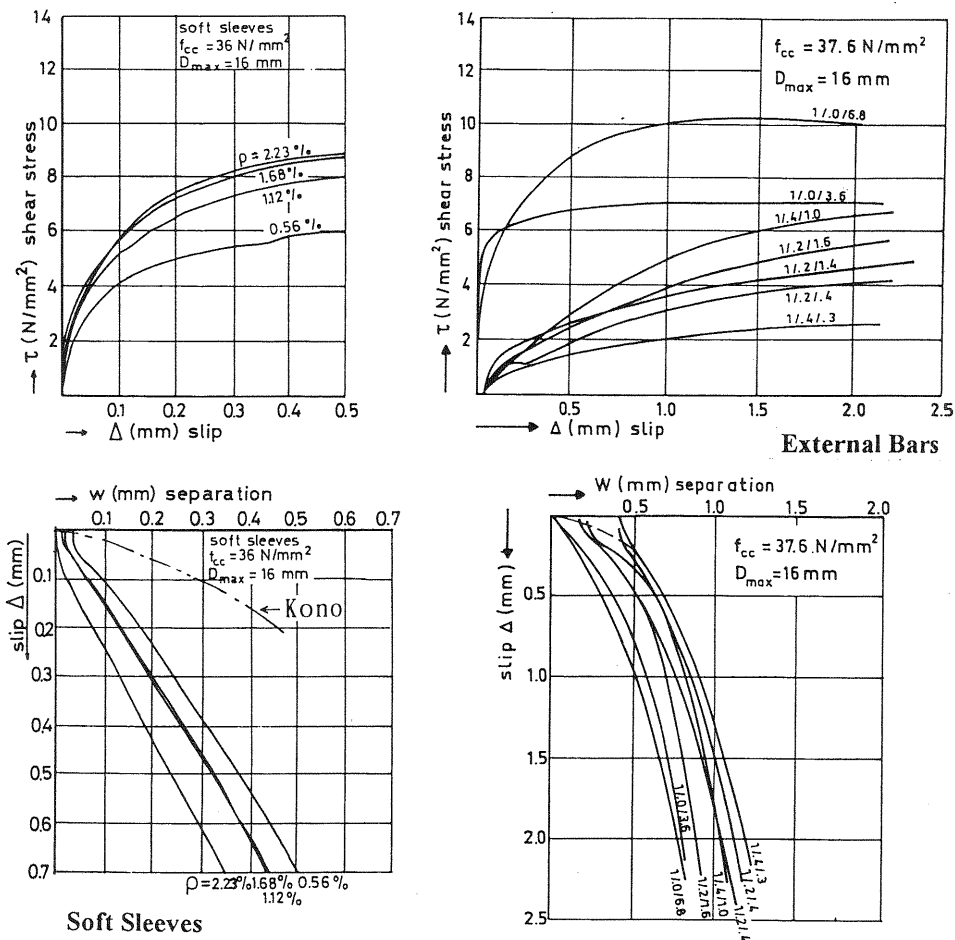

Fig. 9. Comparison of shear-friction and mixed mode fracture results

1438

nominal shear stress on the shearing plane, the separation between crack faces and the slip along the shear plane. Shear stress-slip results were similar for embedded bars with and without soft sleeves even though the slip at a given separation for bars with soft sleeves was almost double that for bars without sleeves. For bars with soft sleeves the curves show responses for differing percentages of uniformly distributed reinforcement crossing the shear plane. For the specimens with external bars the code a/b/c on the curves indicates the mix type / the initial crack width in mm / the normal stress on the crack in MPa for a crack width of 0.6 mm. The most obvious difference between results for specimens with embedded bars and those with external bars is that for external bars small differences in restraint, indicated by the last numeral in the specimen designation, result in different crack opening paths. Further, while slip-separation relationships are essentially linear for specimens with embedded bars, slips increase continuously with increasing separation for specimens with external bars.

Shown on Fig. 9 by broken lines is the slip-CMOD, (s-w), relationship for specimen TH414A specimen. The s-w line for that mixed mode test is similar to the external bar test results. In Kono's tests CMODs ranged between 0.04 and 0.2 mm as inclined cracks formed. For that range in "w" values shear stresses in the external bar tests were very small. Therefore aggregate interlock effects were not to be expected in the mixed mode fracture tests. However, for the same "w" values, the soft sleeve results imply interlock effects would be significant if there was bonded longitudinal reinforcement in the fracture specimens. For 0.56% reinforcement, for example, the 0.06 mm slip that accompanied a CMOD of 0.2 mm for the fracture specimens results in a shear stress of about 3.5 MPa for the soft sleeve specimens. Figure 2 shows that at a CMOD of 0.2 mm the crack had extended 77 mm from the top of the notch. If shear stresses are taken as varying linearly from 3.5 MPa at the crack mouth to zero at the crack tip then TH414A, with bonded reinforcement and a well developed shear crack, would have been able to carry 8.85 KN at a CMOD of 0.2 mm.

5 Concluding remarks

If accurate predictions of the shear behavior of reinforced concrete beams are to be made using fracture mechanics methods, account needs to be taken of the effects of creep and shrinkage on the loads for crack initiation and the effect of bonded reinforcement on controlling crack opening displacements and thus providing aggregate interlock effects.

5 References

Bullington, S.N. (1991) **Fracture in Reinforced Concrete DCB Specimens.** MSCE Thesis, Dept. of Civil Engr., Univ. of Washington, Seattle.

Clark, L.A. and Spiers, D.M. (1978) Tension stiffening in reinforced concrete beams and slabs under short-term load. **Technical Report No.45.521,** Cement and Concrete Association, London, 20p.

Collins, M.P. and Kuchma, D. (1998) How safe are our large, lightly reinforced concrete slabs and footings. **ACI Struct J.,** 95(6).

Collins, M.P., Mitchell, D., Adebar, P. and Vecchio, F.J. (1996) General shear design method. **ACI Struct J.,** 93(1), 36-45.

Kaklauskas, G., Ghaboussi, J. and Hawkins, N.M.(1997) Determination of stress-strain curves for concrete from RC beam tests, in **Modern Building Materials, Structures and Techniques,** University of Vilnius, Lithuania, 138-145.

Kono, S.(1995) **Mixed Mode Fracture of Concrete,** Ph.D. Thesis, Dept. of Civil Engr.., Univ. of Illinois at Urbana-Champaign.

Kono, S., Hawkins, N.M. and Kobayashi, A.S.(1995) Using fracture mechanics concepts to predict the shear strength of concrete structures, in **Proc. Framcos-2,** (Ed. F.H. Wittman), AEDIFICATIO, Freiburg, 1707-1720.

Mihashi, H., Okamura, H. And Bazant, Z.P. (1994) **Size Effect in Concrete Structures.** E & F.N. Spon, London.

Walraven, J.C. (1995) Size effects: their nature and recognition in building codes. **Studi E. Ricerche,** Scuola di Specializzazione in Costruzioni in C.A., Poltecnico di Milano, 16.

Walraven, J.C. and Reinhardt, H.W. (1981) Theory and experiments on the mechanical behaviour of cracks in plain and reinforced concrete subject to shear loading. **Heron,** 26, 1A, 5-68.